Polski Merkuriusz Lekarski

POLISH MEDICAL JOURNAL

ISSN 1426-9686

VOLUME LIII, ISSUE 4, JULY-AUGUST 2025

Polski Merkuriusz Lekarski

POLISH MEDICAL JOURNAL

ISSN 1426-9686

VOLUME LIII, ISSUE 4, JULY-AUGUST 2025

EDITORIAL BOARD

Polski Merkuriusz Lekarski cited by PUBMED/MEDLINE, SCOPUS, INDEX COPERNICUS, EBSCO, POLISH MEDICAL BIBLIOGRAPHY, Ministry of Science and Higer Education.

© **ALUNA PUBLISHING**
29 Z.M. Przesmyckiego St.
05-510 Konstancin-Jeziorna, Poland
tel. +48 604 776 311
a.luczynska@wydawnictwo-aluna.pl

www.polskimerkuriuszlekarski.pl

CONTENTS

ORIGINAL ARTICLES

REVIEW ARTICLES

ORIGINAL ARTICLE

Coronavirus disease 2019 (COVID-19) during pregnancy: Pathomorphological changes in the terminal villi of the placenta

Tetiana V. Savchuk[1], Ivan V. Leshchenko[1], Viktorya V. Vaslovych[2], Oksana H. Chernenko[2], Tetiana A. Malysheva[2]

[1]BOGOMOLETS NATIONAL MEDICAL UNIVERSITY, KYIV, UKRAINE
[2] STATE INSTITUTION «ROMODANOV NEUROSURGERY INSTITUTE NATIONAL ACADEMY OF MEDICAL SCIENCES OF UKRAINE», KYIV, UKRAINE

ABSTRACT

Aim: To investigate the pathomorphological changes in the terminal chorionic villi during COVID-19 in pregnant women.

Materials and Methods: A total of 123 placentas were studied in cases of live term births (groups I) and antenatal asphyxia (groups II). The subgroups were defined as follows: II.2 and I.2 (post-COVID interval of 1–4 weeks); I.1 and II.1 (5–16 weeks). Morphological and statistical research methods were applied.

Results: Spherical structures resembling viral particles were identified in the placenta. In 100 % of the observations, damage to the microcirculatory bed of terminal villi was detected, manifested by cytoplasmic edema of endothelial cells, disruption of cell membranes, nuclear apoptosis and placentitis. With increasing duration of the post-COVID interval, a gradual restoration of endothelial functional activity was observed, evidenced by an increase in laminar microvilli and vesicles, as well as widening of the vascular lumen; whereas in cases of antenatal asphyxia, obliteration of the vascular lumen and stromal fibrosis were noted. A reduction in endothelial cell cytoplasmic edema and stromal edema of terminal chorionic villi was also observed.

Conclusions: The morphogenesis of placental dysfunction in cases of antenatal fetal asphyxia associated with immature protective mechanisms involves endothelial dysfunction, impaired microcirculation, inflammatory infiltration, stromal edema of terminal villi with a reduction in vascular lumen, and subsequent fibrosis. The detection of viral particles with increasing post-COVID interval suggests persistence of SARS-CoV-2, the long-term effects of which on vascular function and its role in the development of placental insufficiency require further investigation.

KEY WORDS: SARS-CoV-2, pregnancy, placenta, pathology

Pol Merkur Lek,2025;53(4):485-494 doi: 10.36740/Merkur202504108

INTRODUCTION

Adequate maternal and fetal perfusion in the placenta is maintained through diffusion exchange across the endothelium, basement membrane, and syncytiotrophoblast cytoplasm – components of the vasculosyncytial membranes [1]. SARS-CoV-2, the causative agent of COVID-19, binds to ACE2 receptors [2, 3], activates endothelial cells, macrophages, and neutrophils, and disrupts microcirculation [4-6]. The birth of polymerase chain reaction (PCR)-negative newborns to COVID-19–positive mothers suggests effective placental defense mechanisms against vertical transmission in late gestation [7]. Nevertheless, cases of antenatal fetal death and placental dysfunction linked to maternal infection have been documented [8, 9]. The identification of irreversible changes in the structures of the vasculosyncytial membranes that contribute to the development of placental dysfunction prompted us to conduct this study.

AIM

The aim of the study was to investigate the pathomorphological changes in terminal chorionic villi during COVID-19 in pregnant women in the second and third trimesters of gestation.

MATERIALS AND METHODS

A total of 123 placentas from pregnant women with confirmed COVID-19 were examined. The mean gestational age in group I was (mean ± standard deviation) 40 ± 1 weeks (n=91), and in group II it was 33 ± 4 weeks (n=32). Group I included cases with live births, while Group II consisted of cases with antenatal asphyxia. Depending on the duration of the post-COVID interval (the time between maternal COVID-19 diagnosis and delivery), subgroups were formed. In subgroups I.1 (n=52) and II.1 (n=11), the post-COVID interval ranged from 5 to 16 weeks; in subgroups I.2 (n=39) and II.2 (n=21), it ranged from 1 to 4 weeks. The condition of newborns in Group I was assessed using the Apgar score, which evaluates heart rate, respiratory effort, muscle tone, reflex irritability, and skin coloration. Placental samples were collected at the Department of Pathological Anatomy of the National specialized children's hospital «OHMATDYT» Ministry of Health of Ukraine during 2020–2022. COVID-19 in pregnant women was confirmed by a positive PCR test for SARS-CoV-2 RNA. PCR testing of live newborns was negative. For comparison, placentas from physiological deliveries before the COVID-19 pandemic were analyzed. The mean gestational age in the control

group was 39 ± 1 weeks (n = 50). The following methods were used: macroscopic, microscopic, electron microscopy (EM), morphometric, and statistical analysis. Tissue sections were stained using standard histological techniques, and immunohistochemistry with monoclonal mouse anti-CD34 antibodies. To visualize full histological tissue sections, digital slides were analyzed using the Pannoramic DESK DW II scanner [10].

To assess quantitative differences in terminal villi (capillaries, stroma), histological images (×630, ×2700) were color-coded in Microsoft Paint (capillaries – black, background – green) and analyzed via ONLINE JPG TOOLS to calculate the color percentage, reflecting the area of the structure [11, 12].

The statistical data analysis was performed by the use of Statistica v. 14.0 (TIBCO Software Inc., USA), IBM SPSS Statistics v. 27.0 (Armonk, NY: IBM Corp., USA), MedStat v. 5.2 and EZR v. 1.68. Quantitative data were presented as median and interquartile range (lower and upper quartiles). Qualitative data were presented as absolute and relative (%) frequency with 95 % confidence intervals. The Kruskal-Wallis test was used to compare the quantitative characteristics of five independent samples, with the following *post hoc* comparisons between the study groups using the Mann-Whitney U test (considering the Bonferroni correction). The qualitative binary data between two independent samples were compared by the use of Fisher`s exact test; between four independent samples by the use of Marascuilo-Liakh-Gurianov procedure. The differences were considered statistically significant at $p < 0,05$ (considering the Bonferroni correction).

RESULTS

We studied the pathomorphological changes in the placenta of live-born infants (Group I) and in the placenta from cases of antenatal fetal asphyxia (Group II), where the mothers had COVID-19 during pregnancy (Table 1). Group II showed a lower gestational age compared with Group I and the control group. In Group I, the course of COVID-19 in the pregnant women was mild in 44 (48,3 %) cases, moderate in 39 (42,9%) cases, and severe (with pneumonia) in 8 (8,8 %) cases. At birth, 64 (70,3 %) newborns had Apgar scores of 8-9 points (normal condition). Twenty-one infants (23,1 %) had scores of 7-8 points, five (5,5 %) had scores of 6-7 points (mild distress), and one (1,1 %) newborn received a score of 3-4 points (severe distress). In Group II, 14 (43,8 %) women had a mild course of COVID-19; 12 (37,5 %) experienced moderate illness, and 6 (18,7%) had a severe form. The incidence of severe COVID-19 was slightly higher in Group II compared to Group I; however, no statistically significant difference was found between the groups. In Group I, no significant correlation was observed between the severity of COVID-19 in pregnant women and the condition of the fetus at birth.

Macroscopic examination of the placenta in the main study groups revealed circulatory disorders in 100% of cases during the acute period of COVID-19 (in subgroups I.2 and II.2), and in 92,3% and 63,6% in subgroups I.1 and II.1, respectively (Table 1): hyperemia, hemorrhages filling cystic cavities (Fig. 1A), and the presence of blood clots on the maternal surface of the placenta. The severity of microcirculatory disturbances decreased with the lengthening of the post-COVID interval. In the case of intrauterine fetal death, placentas in subgroup II.2 exhibited signs of withering and paleness (Fig. 1A), or alternatively, were soaked with dark blood (Fig. 1C, D). Infarctions, predominantly red, were present in subgroups I.2 and II.2. In subgroups I.1 and II.1, infarctions of both types were observed (Fig. 1A, C). The increase in their number was attributed to the organization of red infarcts and fibrinoid deposition in the intervillous space with the prolongation of the post-COVID interval.

Microscopic and EM analysis of the main groups revealed aggregated erythrocytes in the intervillous space and within the lumens of terminal villi blood vessels (Fig. 2D; Fig. 3C, D; Fig. 3D, E), which formed distinctive column-like structures (Fig. 3H). The cytoplasm of endothelial cells in subgroup I.2 was edematous, translucent, with a small number of cytoplasmic ultrastructures (Fig. 2C, D, E). Ruptures in cell membranes were observed (Fig. 2A). Within the vessel lumen, disrupted erythrocytes were detected (Fig. 2A). In one vessel from subgroup I.1, the marginal parts of endothelial cells appeared both electron-dense and translucent. (Fig. 2D, F). Thin-walled vessels with areas of irreversibly damaged endothelial membranes were observed, with ruptured membranes and large cytoplasmic vacuoles replacing destroyed organelles (Fig. 2B). Endothelial cells formed numerous cytoplasmic processes, which in turn created luminal microvilli (arrow) and micropinocytic vesicles. The number of these vesicles was more prominent in subgroup I.1 (Fig. 2C, D; Fig. 3D), whereas in subgroup I.2, only single processes were observed, and desquamated microvilli were seen within the vessel lumen (Fig. 2C). Electron-dense swollen, homogenized mitochondria were seen, along with expansion and splitting of the basal membrane. Apoptotic changes in the nuclei of endothelial cells were evident, with chromatin condensation and invaginations of the nuclear envelope (Fig. 3C).

Numerous acute hemorrhages (subgroups I.2, II.2) and infarctions (subgroups I.1, II.1) led to a reduction in the percentage of free intervillous space. A reduced number of terminal villi was observed in subgroups I.1, II.1, and II.2. In subgroups I.1 and II.1, this was explained by damage to stem villi (endothelial necrosis, vascular thrombosis, stromal fibrosis), which serve as the source for terminal villi formation. In subgroup II.2, the reduction was associated with placental immaturity due to low gestational age. In subgroup I.2, the number of terminal villi did not significantly differ from the control group, which can be explained by the fully developed chorion at the time of infection. Changes in the syncytiotrophoblast included nuclear chromatin condensation and nucleolar disorganization; in the cytoplasm, there was dilation of smooth endoplasmic reticulum cisternae and the formation of numerous vacuoles (Fig. 3E, F). The nuclear envelope of endothelial cells showed multiple protrusions. Changes in microvilli on the surface of the syncytiotrophoblast were noted as a decrease in their number, alteration in shape, shortening, and complete

Table 1. Gestational age, COVID-19 severity, and the pathomorphological changes in the placenta in pregnant women with COVID-19

Parameters		Study groups					p
		Live birth (Group I) (N=91)		Antenatal asphyxia (Group II) (N=32)		Control group (N`=50)	
		Subgroup I.1 (N`=52)	Subgroup I.2 (N`=39)	Subgroup II.1 (N`=11)	Subgroup II.2 (N`=21)		
Gestational age, weeks		40 (39-40)	40 (40-40)	36 (34-37)	31 (30-34)	40 (39-40)	p1-3<0,001 p1-4<0,001 p2-3<0,001 p2-4<0,001 p2-5=0,070 p3-5<0,001 p4-5<0,001
COVID-19 severity, n (%) [95 % CI]	Mild	44 (48,3) [38,1-58,7]		14 (43,8) [26,6-61,7]		-	0,685
	Moderate	39 (42,9) [32,8-53,2]		12 (37,5) [21,2-55,4]		-	0,679
	Severe	8 (8,8) [3,8-15,5]		6 (18,7) [7,0-34,5]		-	0,192
Morphological features							
Stasis, thrombosis, hemorrhage, n (%) [95 % CI]		48 (92,3) [83,4-98,0]	39 (100) [95,2-100]	7 (63,6) [30,7-90,6]	21 (100) [91,3-100]	-	p2-3=0,044
Infarctions, n (%) [95 % CI]		50 (96,2) [89,1-99,7]	13 (33,3) [19,2-49,2]	11 (100) [84,1-100]	21 (100) [91,3-100]	-	p1-2<0,001 p2-3<0,001 p2-4<0,001
Number of terminal villi*		17 (15-18)	26 (25-27)	8 (8-8)	5 (5-6)	26 (25-27)	p1-2<0,001 p1-3<0,001 p1-4<0,001 p1-5<0,001 p2-3<0,001 p2-4<0,001 p3-4<0,001 p3-5<0,001 p4-5<0,001
Stromal edema of terminal villi, n (%) [95 % CI]		50 (96,2) [89,1-99,7]	39 (100) [95,2-100]	10 (90,9) [64,1-100]	21 (100) [91,3-100]	-	0,264
Stromal edema of terminal villi, % of the stromal area		55 (53-56)	71 (67-73)	86 (78-89)	85 (84-87)	32 (30-35)	p1-2<0,001 p1-3<0,001 p1-4<0,001 p1-5<0,001 p2-3<0,001 p2-4<0,001 p2-5<0,001 p3-5<0,001 p4-5<0,001

Table 1. Cont.

Capillary lumen narrowing, % of lumen		46 (44-47)	29 (27-33)	14 (11-22)	15 (13-17)	68 (65-70)	p1-2<0,001 p1-3<0,001 p1-4<0,001 p1-5<0,001 p2-3<0,001 p2-4<0,001 p2-5<0,001 p3-5<0,001 p4-5<0,001
	Chorionamnionitis, n (%) [95 % CI]	47 (90,4) [86,7-96,9]	38 (97,4) [89,9-100]	3 (27,3) [4,5-59,9]	21 (100) [91,3-100]	-	p1-3=0,002 p2-3<0,001 p3-4<0,001
Placentitis	Intervillositis, n (%) [95 % CI]	4 (7,7) [2,0-16,6]	10 (25,6) [13,0-40,8]	11 (100) [84,1-100]	21 (100) [91,3-100]	-	p1-3<0,001 p1-4<0,001 p2-3<0,001 p2-4<0,001
	Basal deciduitis, n (%) [95 % CI]	52 (100) [96,3-100]	39 (100) [95,2-100]	8 (72,7) [40,1-95,5]	21 (100) [91,3-100]	-	<0,001
Capillary lumen narrowing, n (%) [95 % CI]		50 (96,2) [89,1-99,7]	39 (100) [95,2-100]	10 (90,9) [64,1-100]	21 (100) [91,3-100]	-	0,264

*Notes: p_{1-2} – statistical significance of difference between subgroups I.1 and I.2; p_{1-3} – statistical significance of difference between subgroups I.1 and II.1; p_{1-4} – statistical significance of difference between subgroups I.1 and II.2; p_{1-5} – statistical significance of difference between subgroup I.1 and control group; p_{2-3} – statistical significance of difference between subgroups I.2 and II.1; p_{2-4} – statistical significance of difference between subgroups I.2 and II.2; p_{2-5} – statistical significance of difference between subgroup I.2 and control group; p_{3-4} – statistical significance of difference between subgroups II.1 and II.2; p_{3-5} – statistical significance of difference between subgroup II.1 and control group; p_{4-5} – statistical significance of difference between subgroup II.2 and control group; * – number of terminal chorionic villi per field of view at 400× magnification*

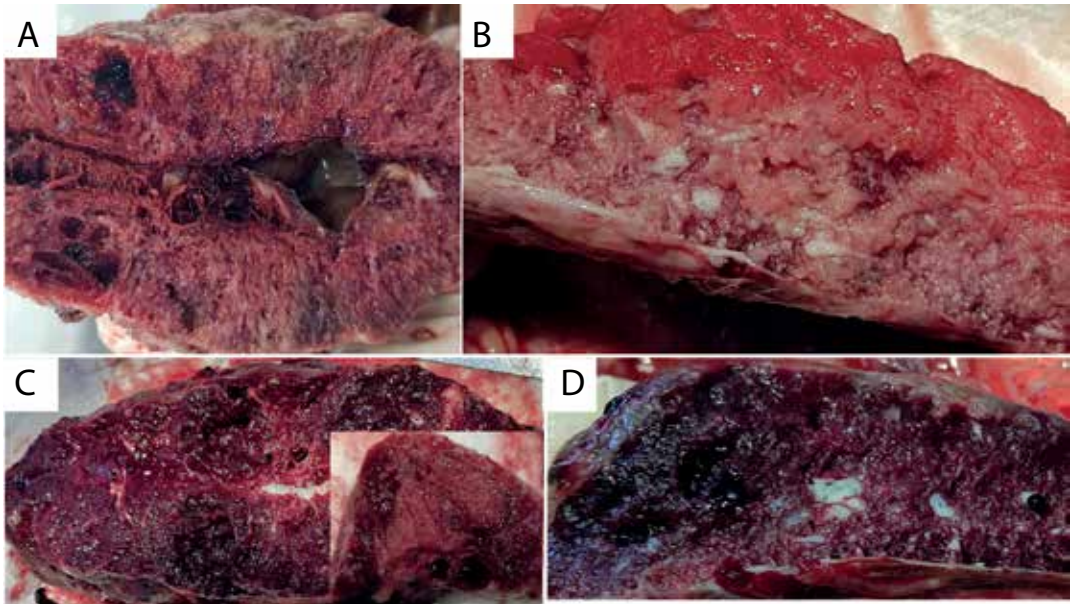

Fig. 1. Pathomorphological changes in the placenta in COVID-19-positive pregnant women. Macroscopic view. A, C – Placenta of a fetus with antenatal asphyxia. B, D – Placenta of a live-born infant at 40 weeks of gestation

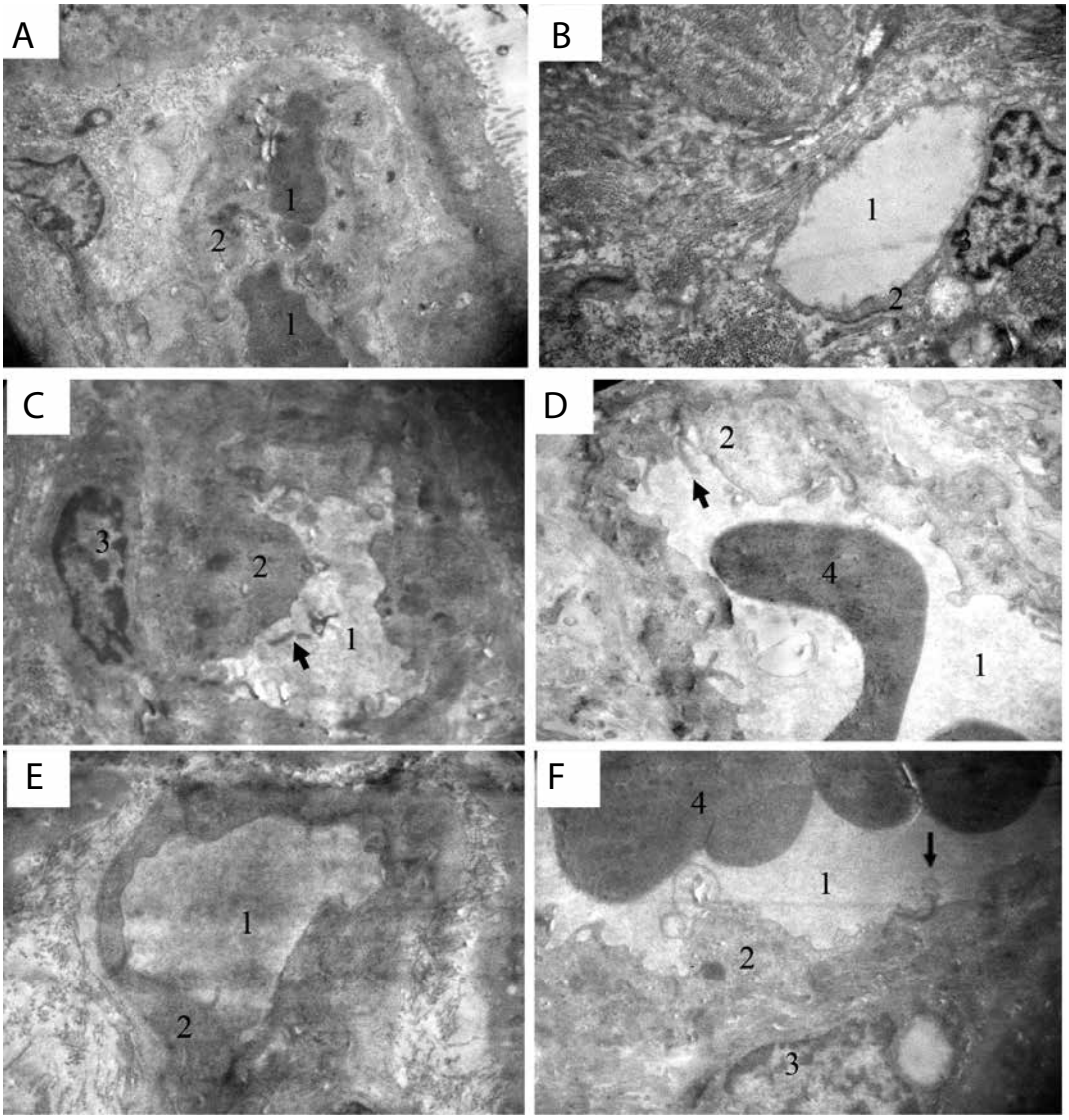

Fig. 2. Microscopic and EM changes in terminal villous vessels in pregnant women with COVID-19 (main groups). A, C, E – subgroup I.2; B, D, F – subgroup I.1. 1 – vessel lumen; 2 – endothelium; 3 – pericyte; 4 – erythrocyte; arrow – microvilli. A ×3000; B, C ×6000; D, E, F ×10000

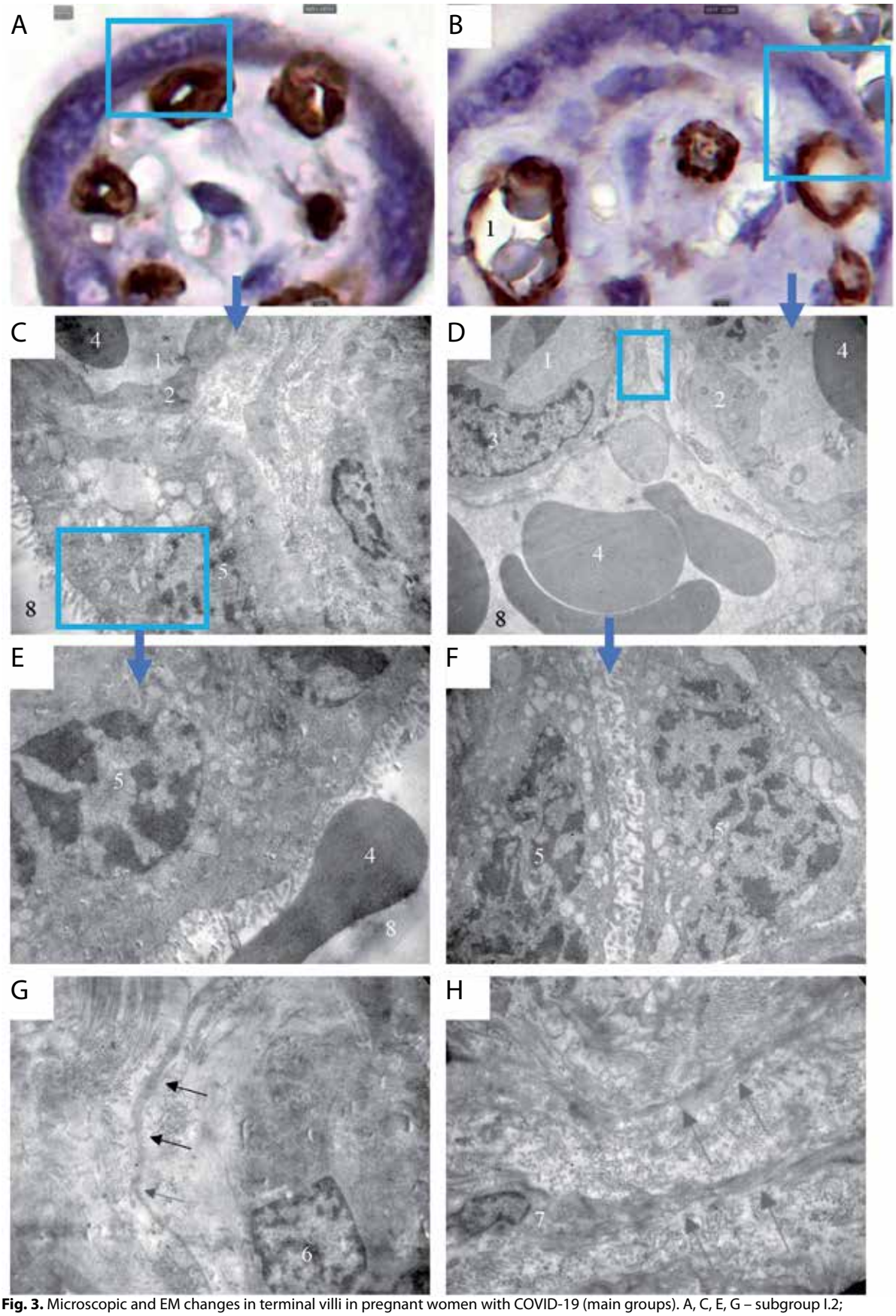

Fig. 3. Microscopic and EM changes in terminal villi in pregnant women with COVID-19 (main groups). A, C, E, G – subgroup I.2; B, D, F, H – subgroup I.1. 1 – vessel lumen; 2 – endothelium; 3 – endothelial cell nucleus; 4 – erythrocyte; 5 – syncytiotrophoblast nucleus; 6 – fibroblast; 7 – telocyte; arrows – telopodes. 8 – intervillous space. A, B – expression of monoclonal anti-CD34 antibodies in endothelial cells of villous arterioles, ×2700. C–H – EM. C, D ×3000; F ×10000; G, E, H ×6000. Blue arrows indicate enlarged views of the structures shown in the squares

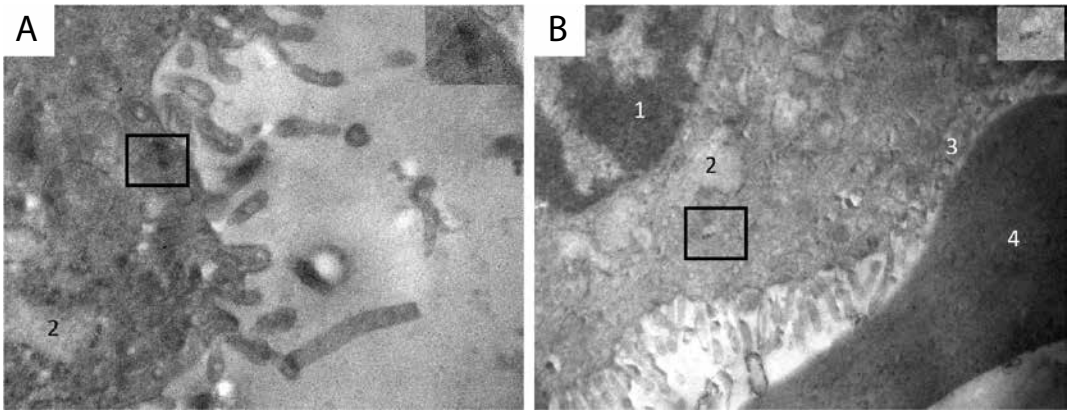

Fig. 4. Ultrastructural changes in the terminal villus of the placenta during the acute phase of COVID-19 in a pregnant woman. 1 – apoptosis of the syncytiotrophoblast nucleus; 2 – enlarged vacuoles in the cytoplasm of the syncytiotrophoblast; 3 – atrophy of microvilli at the site of contact with an erythrocyte; 4 – erythrocyte. Viral particles in the cytoplasm of the syncytiotrophoblast (structures within the black square are shown in the inset), ×10000

loss in areas of hemorrhage, fibrin deposition, or close apposition of terminal villi (Fig. 3D, E, F).

In the terminal villi of the main groups, structures resembling virus-like particles of spherical shape with an osmiophilic membrane were present and were detected near the cell membranes of stromal fibroblasts or syncytiotrophoblasts (Fig. 4A, B).

In the stroma of terminal chorionic villi in mostly all the cases of maternal COVID-19, edema was observed (Fig. 3A, B; Fig. 5B, D), which led to an increased percentage of stromal area in the subgroups. In addition, the studied subgroups were almost entirely represented by the cases of terminal villi capillary lumen narrowing, being the most pronounced in Group II. With an increasing post-COVID interval, a decrease in stromal edema of terminal villi (% of the stromal area) was observed in the subgroup I.1, as compared to the subgroups I.2, II.1 and II.2. This indicated a reduction in edema and was accompanied by restoration of the vascular lumen, as evidenced by an increase in the capillary lumen (Fig. 5A, C). A reduced number of terminal villi (hypoplasia) was noted in subgroups II.1 and II.2 (Table 1). In subgroup II.1, the central localization of capillaries within the chorionic villi was particularly notable (Fig. 5C), which is characteristic of damage to the immature placenta caused by SARS-CoV-2 and may contribute to delayed villous maturation [12].

Electron microscopy of the stromal compartment revealed an increase in collagen fiber content in subgroup I.1 (Fig. 3H) compared to I.2 (Fig. 3G). Fibrin deposits, mucoid and fibrinoid alterations of collagen fibers were observed, manifested by disruption of their compactness and loss of transverse striation, homogenization, and subsequent degradation (Fig. 3G, H).

The amniotic membranes in the main groups appeared thickened and yellowish (Fig. 1B), with microscopic examination revealing chorioamnionitis. It was observed in 90,4% of subgroup I.1, 97,4% of subgroup I.2, 27,3% of subgroup II.1, and 100% of subgroup II.2. Basal deciduitis was observed in 100% of subgroups I.1, I.2 and II.2, and 72,7% of subgroup II.1. Intervillositis was found in 25,6% of subgroup I.2, and in 100% of cases with antenatal fetal asphyxia during the acute phase of COVID-19 (Table 1).

DISCUSSION

Cases of COVID-19 in pregnant women resulting in live births and intrauterine fetal death were analyzed. The condition of the fetus at birth was found to be dependent on the severity of placental pathological changes caused by SARS-CoV-2 [13, 14]. No statistically significant correlation was found between the severity of COVID-19 in pregnant women and the fetal condition at birth [15], which can be attributed to the absence of a consistent association between the maternal clinical status and the placental pathological changes induced by the infection.

Our study focused on morphological changes in components forming the vasculosyncytial membranes: endothelium, stroma, and syncytiotrophoblast. In 100% of our cases, during the acute phase of COVID-19 in pregnant women, microcirculatory damage in the terminal villi was observed, manifested by endothelial cell cytoplasmic edema, membrane rupture, and irreversible endothelial damage. Edema and microvilli desquamation caused by SARS-CoV-2 were signs of endothelial dysfunction [4]. With an increase in the post-COVID interval, restoration of the functional activity of the endothelium was observed (subgroup I.1), as evidenced by an increase in the number of microvilli and micropinocytic vesicles on the luminal surface of endothelial cells. Direct viral action on endothelial cells (aponecrosis) or cytokine-mediated effects triggered by SARS-CoV-2 can lead to a preeclampsia-like syndrome in COVID-19-positive pregnant women [15]. According to researchers, apoptotic changes in the nuclei and cytoplasm of endothelial cells and circulatory disturbances impair fetal perfusion [16]. During the acute phase, vascular lumens were obstructed with destroyed erythrocytes, resulting in a reduced number of vessels in the villi (subgroup II.1). In subgroup I.1, gradual restoration of vessel lumen and an increase in their percentage was noted. As the post-COVID interval increased, a reduction in

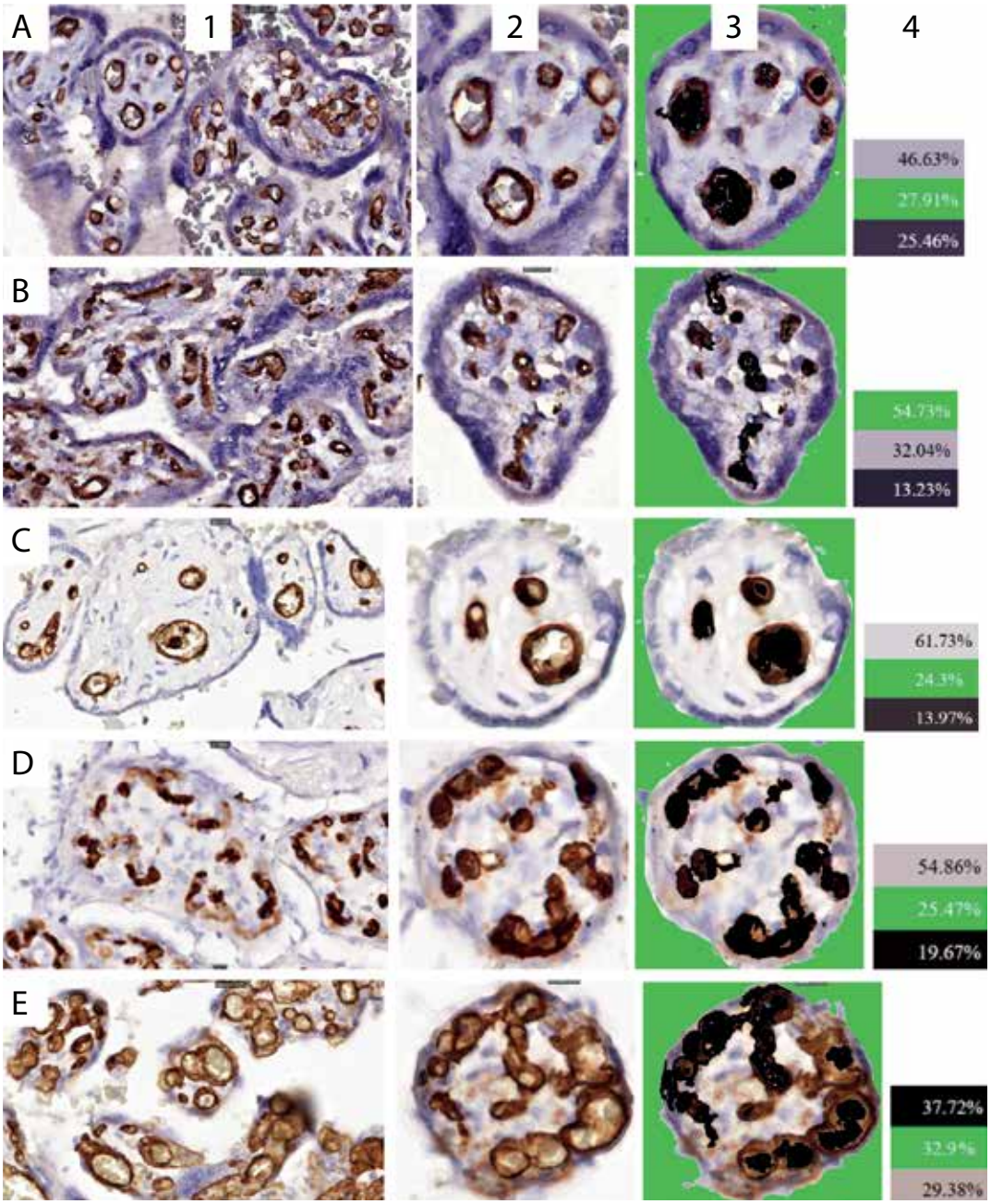

Fig. 5. Microscopic structural changes in the placenta during COVID-19 – 1. Representative placentas: A – subgroup I.1; B – subgroup I.2; C – subgroup II.1; D – subgroup II.2 and in the comparison group – E. Expression of monoclonal antibodies against CD34 in the endothelium of villous arterioles, ×630. 2 (A–E): Terminal villi, ×1200 – quantitative assessment of vascular and stromal percentages in histological sections of terminal villi. 3 (A–E): Lumen of vessels (black) and background surrounding the villi (green) colored using Microsoft Paint. 4 (A–E): the percentages of dominant colors in the images were determined using the ONLINE JPG TOOLS service, with each color corresponding to the proportional area of the analyzed structures: vessels (black), stroma (gray), and background (green)

cytoplasmic edema of endothelial cells and stromal edema in the terminal chorionic villi was observed. However, despite these improvements, stromal edema remained until delivery, contributing to thickening of the vasculosyncytial membrane compared to the control group [16].

Edema led to increased thickness of the vasculosyncytial membranes (central location of vessels), which caused malperfusion [11, 12]. The thickening of the vasculosyncytial membranes contributes to pathological endothelial activation, and the substances they produce lead to impaired microcirculation in the vascular lumen, vasoconstriction, stromal edema, hypoxia, and fibroblast activation, ultimately resulting in fibrosis [4]. The presence of apoptotic syncytiotrophoblasts, endothelial cells indicate an energy deficit caused by cytokine storm and tissue hypoxia, which activates fibroblasts.

Viral particles were detected by EM both in the acute phase of COVID-19 and in cases from subgroup I.1. Spherical particles

were localized in the villous stroma and in the cytoplasm of the syncytiotrophoblast. Our data align with other researchers who have reported extracellular viral particles [3]. Although placental pathological changes such as the presence of viral particles, placentitis, and malperfusion were observed during late gestation in COVID-19 cases, neonates were born PCR-negative and without clinical signs of hypoxia, even when delivered by PCR-positive mothers [13]. This is associated with protective mechanisms against vertical transmission of the virus [2, 3]. Placentitis of varying degrees of severity was detected in placentas from the main groups. The intensity of inflammatory manifestations declined with increasing post-COVID interval duration. Generalized intervillositis was observed predominantly in subgroup II.2, which was explained by the immaturity of the placental protective mechanisms and was the cause of antenatal fetal death [12].

CONCLUSIONS

The morphogenesis of placental dysfunction in cases of antenatal fetal asphyxia associated with immature protective mechanisms involves endothelial dysfunction, impaired microcirculation, inflammatory infiltration, stromal edema of terminal villi with a reduction in vascular lumen, and subsequent fibrosis.

In the placentas of live-born infants, an increasing post-COVID interval was associated with restoration of the vascular lumen in the terminal chorionic villi and a reduction in the severity of placentitis (subgroup I.1).

The presence of viral particles with an increasing post-COVID interval indicates SARS-CoV-2 persistence, the prolonged impact of which on vascular function and its role in the development of placental insufficiency requires further investigation.

REFERENCES

1. Sankar KD, Bhanu PS, Kiran S et al. Vasculosyncytial membrane in relation to syncytial knots complicates the placenta in preeclampsia: a histomorphometrical study. Anat Cell Biol. 2012;45(2):86-91. doi: 10.5115/acb.2012.45.2.86.
2. Beyerstedt S, Casaro EB, Rangel ÉB. COVID-19: angiotensin-converting enzyme 2 (ACE2) expression and tissue susceptibility to SARS-CoV-2 infection. European Journal of Clinical Microbiology & Infectious Diseases. 2021;40(5):905-919. doi: 10.1007/s10096-020-04138-6.
3. Bryce C, Grimes Z, Pujadas E et al. Pathophysiology of SARS-CoV-2: the Mount Sinai COVID-19 autopsy experience. Mod Pathol 2021;34:1456-1467 doi: 10.1038/s41379-021-00793-y.
4. Deanfield JE, Halcox JP, Rabelink TJ. Endothelial Function and Dysfunction. Circulation. 2007;115(10):1285-1295. doi: 10.1161/CIRCULATIONAHA.106.652859.
5. Baergen RN, Heller DS. Placental Pathology in Covid-19 Positive Mothers: Preliminary Findings. Pediatric and Developmental Pathology. 2020;23(3):177-180. doi: 10.1177/1093526620925569.
6. Tian X, Li C, Huang A et al. Potent binding of 2019 novel coronavirus spike protein by a SARS coronavirus-specific human monoclonal antibody. Emerging Microbes & Infections. 2020;9(1):382-385. doi: 10.1080/22221751.2020.1729069.
7. Turyanytsya SM, Korchins'ka OO, Sabova AV et al. Vplyv gostroho respiratornoho virusnoho zakhvoryuvannya SARS-Cov2-19 na perebih vagitnosti ta polohiv. [Influence of SARS-CoV-2 acute respiratory viral disease on pregnancy and childbirth]. Reproduktyvne zdorov'ya zhinky. 2021;2(47):15-18. doi: 10.30841/2708-8731.2.2021.232515. (Ukrainian)
8. Galang RR, Chang K, Strid P et al. Severe Coronavirus Infections in Pregnancy: A Systematic Review. Obstetrics & Gynecology. 2020;136(2):262-272. doi: 10.1097/AOG.0000000000004011.
9 Hsu AL, Guan M, Johannesen E et al. Placental SARS-CoV-2 in a pregnant woman with mild COVID-19 disease. Journal of Medical Virology. 2020;93(2):1038-1044. doi: 10.1002/jmv.26386.
10. Aeffner F, Zarella MD, Buchbinder N et al. Introduction to Digital Image Analysis in Whole-slide Imaging: A White Paper from the Digital Pathology Association. Journal of pathology informatics. 2019;10(1):9. doi: 10.4103/jpi.jpi_82_18.
11. Savchuk T. Patomorfologichni zminy platsenty v gostromu periodi COVID-19 u vahitnykh. [Pathomorphological changes of the placenta in the acute period of COVID-19 in pregnant women]. Skhidnoukrayins'kyy medychnyy zhurnal. 2024;12(2):323-334. doi: 10.21272/eumj.2024;12(2):323-334. (Ukrainian)
12. Savchuk T. Pathomorphological changes of the placenta in coronavirus disease (COVID-19) in pregnant women at 19-32 weeks of gestation. Proceeding of the Shevchenko Scientific Society. Medical Sciences. 2024;73(1). doi: 10.25040/ntsh2024.01.16.
13. Savchuk TV. Patomorfologichni zminy platsenty pry koronavirusnii khvorobi (COVID-19) u vahitnykh u druhomu ta tretomu trymestrakh hestatsii. [Pathomorphological changes of the placenta in coronavirus disease (COVID-19) in pregnant women in the second and third trimesters of pregnancy]. Medicni Perspektivi. 2024;29(4):84-94. doi: 10.26641/2307-0404.2024.4.319224. (Ukrainian)
14. Levitan D, London V, McLaren RA et al. Histologic and Immunohistochemical Evaluation of 65 Placentas From Women With Polymerase Chain Reaction-Proven Severe Acute Respiratory Syndrome Coronavirus 2 (SARS-CoV-2) Infection. Archives of Pathology & Laboratory Medicine. 2021;145(6):648-656. doi: 10.5858/arpa.2020-0793-SA.
15. Mendoza M, Garcia-Ruiz I, Maiz N et al. Pre-eclampsia-like syndrome induced by severe COVID-19: a prospective observational study. BJOG: An International Journal of Obstetrics & Gynaecology. 2020;127(11):1374-1380. doi: 10.1111/1471-0528.16339 .
16. Giordano G, Petrolini C, Corradini E et al. COVID-19 in pregnancy: placental pathological patterns and effect on perinatal outcome in five cases. Diagnostic Pathology. 2021; 16(1):88. doi: 10.1186/s13000-021-01148-6.

The work is a fragment of scientific research work of the Department of Pathological Anatomy, Bogomolets National medical university, Kyiv, Ukraine: "Morphogenesis Research and Optimization of Morphological Diagnostics of the Most Prevalent Socially Significant Diseases"" (registration number 0124U000022). Planned duration of the research project: 2024 to 2026."

The study was approved by the local bioethical committee of the Bohomolets National Medical University (protocol No 144 of 29.03.2021), and was carried out in accordance with the principles outlined in the Declaration of Helsinki. All participants provided written informed consent.

CONFLICT OF INTEREST

The Authors declare no conflict of interest

CORRESPONDING AUTHOR:
Tetiana V. Savchuk
Department of Pathological Anatomy
Bohomolets National Medical University
13 T. Shevchenko Blvd., 01601 Kyiv, Ukraine
e-mail: t.savchuk@nmu.ua

ORCID AND CONTRIBUTIONSHIP

Tetiana V. Savchuk: 0000-0002-7218-0253 A B C D E F
Ivan V. Leshchenko: 0000-0001-8239-256X A B C
Viktoriya V. Vaslovych: 0000-0002-7503-4547 A D
Oksana H. Chernenko: 0000-0001-6292-8339 A B
Tetyana A. Malysheva: 0000-0003-4071-8327 D E F

A – Work concept and design, B – Data collection and analysis, C – Responsibility for statistical analysis, D – Writing the article, E – Critical review, F – Final approval of the article

RECEIVED: 14.01.2025
ACCEPTED: 27.06.2025